

# Light-Harvesting Complex 1 Stabilizes $P^+Q_B^-$ Charge Separation in Reaction Centers of *Rhodobacter sphaeroides*<sup>†</sup>

Francesco Francia,<sup>\*,‡</sup> Manuela Dezi,<sup>‡</sup> Alberto Rebecchi,<sup>‡</sup> Antonia Mallardi,<sup>§</sup> Gerardo Palazzo,<sup>||</sup> Bruno Andrea Melandri,<sup>‡</sup> and Giovanni Venturoli<sup>‡,⊥</sup>

Dipartimento di Biologia, Laboratorio di Biochimica e Biofisica, Università di Bologna, 40126 Bologna, Italy, Istituto per i Processi Chimico-Fisici, CNR, 70126 Bari, Italy, Dipartimento di Chimica, Università di Bari, 70126 Bari, Italy, and Istituto Nazionale per la Fisica della Materia, UdR di Bologna, 40127 Bologna, Italy

Received June 30, 2004; Revised Manuscript Received September 6, 2004

**ABSTRACT:** The kinetics of charge recombination following photoexcitation by a laser pulse have been analyzed in the reaction center–light harvesting complex 1 (RC–LH1) purified from the photosynthetic bacterium *Rhodobacter sphaeroides*. In RC–LH1 core complexes isolated from photosynthetically grown cells  $P^+Q_B^-$  recombines with an average rate constant,  $\langle k \rangle \approx 0.3 \text{ s}^{-1}$ , more than three times smaller than that measured in RC deprived of the LH1 ( $\langle k \rangle \approx 1 \text{ s}^{-1}$ ). A comparable, slowed recombination kinetics is observed in RC–LH1 complexes purified from a *pufX*-deleted strain. Slowing of the charge recombination kinetics is even more pronounced in RC–LH1 complexes isolated from wild-type semiaerobically grown cells ( $\langle k \rangle \approx 0.2 \text{ s}^{-1}$ ). Since the kinetics of  $P^+Q_A^-$  recombination is unaffected by the presence of the antenna, the  $P^+Q_B^-$  state appears to be energetically stabilized in core complexes. Determinations of the ubiquinone-10 ( $UQ_{10}$ ) complement associated with the purified RC–LH1 complexes always yield  $UQ_{10}/RC$  ratios larger than 10. These quinone molecules are functionally coupled to the RC–LH1 complex, as judged from the extent of exogenous cytochrome  $c_2$  rapidly oxidized under continuous light excitation. Analysis of  $P^+Q_B^-$  recombination, based on a kinetic model which considers fast quinone equilibrium at the  $Q_B$  binding site, indicates that the slowing down of charge recombination kinetics observed in RC–LH1 complexes cannot be explained solely by a quinone concentration effect and suggests that stabilization of the light-induced charge separation is predominantly due to interaction of the  $Q_B$  site with the LH1 complex. The high  $UQ_{10}$  complements detected in RC–LH1 core complexes, but not in purified light-harvesting complex 2 and in RC, are proposed to reflect an in vivo heterogeneity in the distribution of the quinone pool within the chromatophore bilayer.

The transduction of light energy into a proton electrochemical potential is the peculiar characteristic of photosynthetic organisms. In *Rhodobacter (Rb.)*<sup>1</sup> *sphaeroides*, a member of proteobacteria  $\alpha$ -subgroup, the interaction between several membrane complexes and their soluble partners

leads to the formation of a light-induced proton gradient across the plasma membrane.

Light energy is mainly absorbed by light-harvesting (LH) antenna complexes which funnel excitation to the reaction center (RC) (1). Two kinds of antenna (LH1 and LH2) are present in *Rb. sphaeroides*. LH1 and the RC are intimately associated to form the so-called core complex, whereas the peripheral LH2 transfers the energy to the RC only via the LH1 complex (2). Both LH1 and LH2 are composed of two small polypeptides,  $\alpha$  and  $\beta$ , which bind bacteriochlorophyll (BChl) and carotenoids (3). The *Rb. sphaeroides* LH2 is built from nine  $\alpha\beta$  heterodimers arranged to form a closed circle; LH1 shows a similar circular arrangement of dimeric subunits, but with an increased number of  $\alpha\beta$  heterodimers. The increased diameter of the resulting ring-like structure allows the LH1 to locate inside the RC, forming the core complex (4). In *Rb. sphaeroides* the core complex includes an additional small protein, called PufX, which is required for the photosynthetic phenotype under physiological condition of growth (5). Biochemical (6, 7) and low-resolution crystallographic data (8–10) indicate that the presence of PufX decreases the number of LH1  $\alpha\beta$  heterodimers in the

<sup>†</sup> The financial support of MIUR of Italy is acknowledged by F.F., B.A.M., and G.V. (Grant PRIN/2003, Bioenergetica: genomica funzionale, meccanismi molecolari ed aspetti fisiopatologici; Grant FIRB/2001, Meccanismi molecolari della fotosintesi) and by G.P. (Grant PRIN/2003, Nuovi biosensori basati su neurorecettori immobilizzati). M.D. gratefully acknowledges a fellowship from MIUR (FIRB/2001). G.P. was supported by the Consorzio Interuniversitario per lo sviluppo dei Sistemi a Grande Interfase (CSGI-Firenze). F.F. was also supported by A. M. Contiglozzi and A. Contiglozzi.

\* Corresponding author. Phone +39-051-2091300. Fax: +39-051-242576. E-mail: francia@alma.unibo.it.

<sup>‡</sup> Università di Bologna.

<sup>§</sup> Istituto per i Processi Chimico-Fisici, CNR.

<sup>||</sup> Università di Bari.

<sup>⊥</sup> Istituto Nazionale per la Fisica della Materia (INFN).

<sup>1</sup> Abbreviations: *Rb.*, *Rhodobacter*; LH, light harvesting; RC, reaction center; BChl, bacteriochlorophyll; UQ, ubiquinone; P, primary electron donor;  $Q_A$ , primary ubiquinone acceptor;  $Q_B$ , secondary ubiquinone acceptor; cyt, cytochrome; WT, wild type; PMC, photosynthetic membrane complex; OG, *n*-octyl  $\beta$ -D-glucopyranoside; LDAO, lauryldimethylamine *N*-oxide; DAD, diaminodurene.

core complex, interrupts the LH1 ring, and switches the RC–LH1 supramolecular organization from a monomeric to a dimeric structure.

Within the RC complex, direct photon absorption or energy transfer from LH1 promotes the primary electron donor P (a special pair of bacteriochlorophylls) to the first excited singlet state  $P^*$ , from which an electron is transferred, via a bacteriopheophytin, to a first ubiquinone-10 ( $UQ_{10}$ ) molecule,  $Q_A$ , generating the primary charge-separated state  $P^+Q_A^-$ . The electron is then delivered from  $Q_A^-$  to a second ubiquinone-10 molecule at the  $Q_B$  site. In the absence of an electron donor to  $P^+$  the electron on  $Q_B^-$  recombines with the hole on  $P^+$  (11). In the presence of the physiological electron donor to  $P^+$  [a soluble cytochrome (cyt)  $c_2$ ], a new excitation of P leads to the full reduction and protonation of  $Q_B$  to  $UQH_2$ , which dissociates from the  $Q_B$  site and is replaced by oxidized ubiquinone from a pool present in stoichiometric excess over the RC (12, 13). The cytochrome  $bc_1$  complex utilizes ubiquinol and oxidized cyt  $c_2$  as reductant and oxidant, respectively, with the net result of this cyclic electron transfer chain acting as a proton pumping system from the cytoplasmic side of the membrane to the periplasmic space (12).

During the past decades RC charge transfer events have been mainly analyzed in purified RCs lacking the antenna complex LH1 (hereafter called RC-only complexes). With the availability of the X-ray diffraction structure at atomic resolution (14–17) RC-only complexes from *Rb. sphaeroides* have become a paradigmatic system in the study of intramolecular electron transfer as well as of the interaction of quinone cofactor with electron transfer complexes. Although many basic aspects of these processes have been elucidated by studies performed on RC-only complexes, it is expected that the in vivo functional properties of the RC itself are significantly modulated by the integration of the RC complex into a supramolecular structure of higher complexity. An important example, recently come to light, is the facilitation of the  $UQH_2/UQ$  exchange at the  $Q_B$  site of the RC promoted by the PufX protein and due to its role in structurally organizing the RC–LH1 complex (18). Non-systematic data in the literature also indicate that the kinetics of electron transfer reactions in RC-only suspensions and in a more intact system (chromatophore vesicles) may differ considerably, both in the case of intraprotein processes [e.g.,  $P^+Q_B^-$  recombination (19, 20)] and in the case of interprotein electron transfer [e.g., cyt  $c_2$  oxidation by  $P^+$  (21, 22)].

In a first step to fill the gap between the in vivo and RC-only functional properties, the core RC–LH1 complex of *Rb. sphaeroides* appears to be a suitable intermediate system, also in view of the structural information made recently available for this complex at low resolution in *Rb. sphaeroides* (8–10) and, at 4.8 Å resolution, in the related species *Rhodospseudomonas palustris* (23).

In the present paper we have compared the recombination kinetics of the state  $P^+Q_AQ_B^-$  induced by a laser actinic pulse in RC-only and in RC–LH1 core complexes. This reaction has been extensively characterized in RC-only complexes, yielding a wealth of information on the energetics of the electron transfer events involving the primary and secondary quinone acceptors (see, e.g., refs 19, 24, and 25) and on the binding of quinone at the  $Q_B$  site (see, e.g., refs 26 and 27). Within the core complexes  $P^+Q_AQ_B^-$  recombination is found

to be markedly slower (from three to four times) than observed in RC-only complexes. Determination of the  $UQ_{10}$  complement of the purified RC–LH1 complexes revealed a surprisingly large pool of quinone molecules, competent as efficient electron acceptors from  $Q_A^-$ , indicating that more than one-third on the whole quinone membrane pool is functionally associated with the isolated core complex. This high  $UQ_{10}$  concentration cannot, however, account for the observed slowing of charge recombination, which is interpreted as reflecting a sizable stabilization of the electron on  $Q_B$  due to interaction with the LH1 complex surrounding the RC.

## MATERIALS AND METHODS

**Bacterial Growth.** *Rb. sphaeroides* strains and the plasmid used in this work are described in ref 7. We call wild type (WT) and  $X^-$ , respectively, strains carrying the *puf* operon either complete or deleted of the *pufX* gene onto a low copy number plasmid. The growth conditions and the antibiotics used are also described in ref 7. For photosynthetic cultures, each 1 L Roux bottle was placed in a 30 °C water bath, inoculated with 50 mL of preculture, and illuminated by two 100 W tungsten bulb lamps.

**RC, RC–LH1, LH2, and Cytochrome  $c_2$  Purification.** Chromatophores were isolated as described in ref 28, frozen in liquid nitrogen, and stored at –80 °C. Photosynthetic membrane complexes (LH2, dimeric and monomeric forms of RC–LH1) were isolated by using essentially the differential solubilization protocol described in ref 7. After removal of peripheral membrane proteins with sodium bromide, photosynthetic membrane complexes (PMC) were solubilized using 3% *n*-octyl  $\beta$ -D-glucopyranoside (OG) and 0.5% sodium cholate. The detergent extract was separated by zone centrifugation over a sucrose density gradient (10–40% w/w) containing 0.6% OG and 0.2% sodium cholate. LH2 and dimeric LH1–RC complexes were collected from the fractions termed respectively PMC1 and PMC4 in ref 7. In the extract from the  $X^-$  strain, only monomeric LH1–RC complexes are present (fraction PMC3 in ref 7). Sucrose removal was obtained by eluting the collected suspensions of photosynthetic complexes through a PD10 (Pharmacia, Sweden) column with 50 mM glycylglycine, 0.6% OG, and 0.2% sodium cholate, pH 7.8.

Reaction centers lacking the antenna system (RC-only) were purified from *Rb. sphaeroides* R26 according to ref 29. To replace the detergent lauryldimethylamine *N*-oxide (LDAO) with OG and sodium cholate, the LDAO suspension of purified RCs was first diluted below the critical LDAO micellar concentration and then eluted through a PD10 column with 50 mM glycylglycine, 0.6% OG, and 0.2% sodium cholate, pH 7.8. The effectiveness of this OG/LDAO exchange procedure was tested by verifying that, following the exchange treatment, no increase in turbidity was induced upon acidification at pH = 6.5. Emulsification of the protein, occurring at acidic pHs in LDAO but not in OG suspensions of RCs, has been recently characterized (30). Cytochrome  $c_2$  was isolated following the protocol described by Bartsch (31), slightly modified as detailed in ref 32.

**HPLC Determination of Quinone Content.** For the evaluation of the quinone content of chromatophores and purified photosynthetic membrane complexes, 250  $\mu$ L of the respec-

tive preparations was extracted as reported in ref 33. The dried extract was resuspended in 500  $\mu\text{L}$  of 2-propanol, and 20  $\mu\text{L}$  of the obtained solution was injected in a Jasco Pu 1580 HPLC apparatus equipped with a Waters C-18 reverse-phase column (Waters Spherisorb 5  $\mu\text{M}$  ODS2, 4.6  $\times$  250 mm); a mixture of 99.5% ethanol and 0.5% water (plus 1 mL/L  $\text{HClO}_4$ , 65%) at a flow rate of 1 mL/min was used as mobile phase. The detection wavelength was 275 nm (Jasco UV-970 detector). Calibration curves were obtained by injecting solutions of oxidized ubiquinone-10 (from Sigma-Aldrich) at the appropriate concentrations.

**Characterization of Chromatophores and of Purified Photosynthetic Membrane Complexes.** The concentration of photoactive RCs in chromatophores or in isolated core complexes was evaluated by flash spectrophotometry essentially as described in ref 7. Chromatophores were suspended in 50 mM glycylglycine and 100 mM KCl at pH 7.8, and the total concentration of photooxidizable primary donor P was measured from the absorbance change induced at 605–542 nm by a train of eight flashes fired at 10 Hz frequency. Actinic flashes were provided by a xenon lamp (EG&G FX201, discharging a 3  $\mu\text{F}$  capacitor charged at 1.5 kV) with a pulse duration at half-maximal intensity of 4  $\mu\text{s}$ , screened through two layers of Wratten 88A gelatin filter. The cytochrome  $bc_1$  complex was inhibited with 10  $\mu\text{M}$  antimycin A and 0.5  $\mu\text{M}$  mixotyzol; 10  $\mu\text{M}$  valinomycin and 10  $\mu\text{M}$  nigericin were also added to collapse the transmembrane proton gradient and to avoid spectral interference due to BChl and carotenoid electrochromic bandshifts. Analogous measurements on RC–LH1 complexes were performed directly on the suspensions eluted from the PD10 column (i.e., in 50 mM glycylglycine, 0.6% OG, and 0.2% sodium cholate, pH 7.8). During averaging cycles, samples were dark adapted for 4 min to allow full recovery of the photooxidized RC. The concentration of RC in RC-only preparations was determined spectrophotometrically by the absorbance at 802 nm, using an extinction coefficient  $\epsilon_{802} = 288 \text{ mM}^{-1} \text{ cm}^{-1}$  (34). In these preparations, the concentration of photooxidizable primary donor was evaluated from the absorbance change induced at 605 nm by continuous light excitation using  $\Delta\epsilon = 19.5 \text{ mM}^{-1} \text{ cm}^{-1}$  (35, 36). Continuous photoactivation was provided by a collimated 200 W quartz halogen lamp as described in ref 37. RC and  $\text{P}^+$  concentrations estimated by the procedures described above agreed within the experimental error.

To determine the BChl/ $\text{P}^+$  stoichiometry in chromatophores, purified RC-only, and RC–LH1 preparations, a volume of 50  $\mu\text{L}$  of the same samples used in the spectrophotometric determination of  $\text{P}^+$  was extracted in 1 mL of an acetone–methanol (7:2) mixture, and the BChl concentration was evaluated spectrophotometrically according to Clayton (38). The concentration of LH2 complexes purified over the sucrose density gradient (PMC1; see above) was evaluated on the basis of the BChl concentration of the fraction, assuming a stoichiometry of 27 BChl molecules per LH2 complex (39).

Photooxidation of exogenous cyt  $c_2$  by RC-only and RC–LH1 complexes under continuous light was monitored at 551 nm using an extinction coefficient of  $19.5 \text{ mM}^{-1} \text{ cm}^{-1}$  (35, 36).

**Charge Recombination Kinetics.** The kinetics of charge recombination were measured by flash absorption spectro-

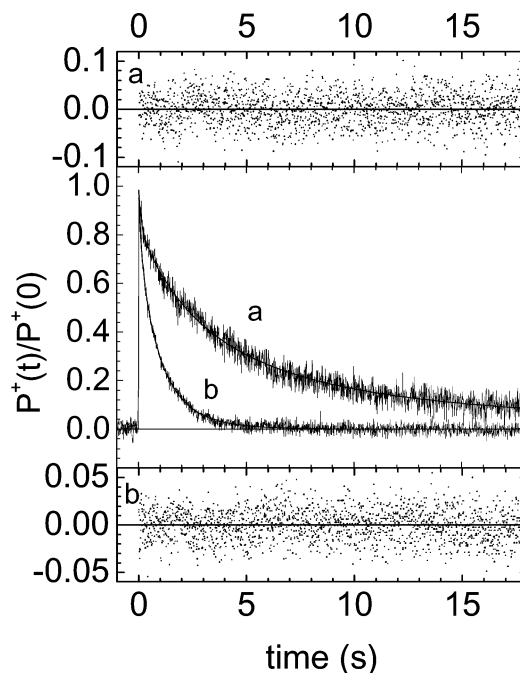


FIGURE 1: Kinetics of charge recombination following flash excitation in dimeric RC–LH1 complexes purified from photosynthetically grown cells (trace a) and in RC-only complexes (trace b). Measurements, performed at  $T = 298 \text{ K}$ , in the presence of 0.6% OG and 0.2% sodium cholate, are the result of four averages.  $\text{P}^+$  decays recorded at 605 nm have been normalized to the maximal amplitude at the time of the laser pulse ( $t = 0$ ). Traces have been fitted to the sum of an exponential decay (fast phase) and a power law (slow phase) as described in detail in the text (see eq 1). This procedure yielded  $\langle k \rangle = 0.28 \text{ s}^{-1}$  (0.25, 0.31) and  $\sigma = 0.22 \text{ s}^{-1}$  (0.19, 0.26) in the RC–LH1 complex and  $\langle k \rangle = 1.01 \text{ s}^{-1}$  (0.97, 1.06) and  $\sigma = 0.35 \text{ s}^{-1}$  (0.28, 0.41) in RC-only. Values in parentheses represent the extremes of confidence intervals within one standard deviation. Residues for traces a and b are shown in the upper and lower panels, respectively.

photometry using an apparatus of local design (27). The rereduction of  $\text{P}^+$  following a laser actinic pulse was monitored at 605, 542, and 420 nm, obtaining essentially the same kinetics. Samples were photoactivated by a 20 ns pulse from a dye laser cavity (RDP-1; Radiant Dyes GmbH, Wermelskirchen, Germany) pumped by a frequency-doubled Q-switched Nd:YAG laser (Surelite 10; Continuum, Santa Clara, CA). Styryl 9 was used as a dye ( $\lambda_{\text{max}}$  at 810 nm). Samples were dark adapted for at least 4 min between each measurement. To check the stability of semiquinone formed upon flash excitation at the  $\text{Q}_\text{B}$  site, semiquinone formation and decay were monitored at 446 nm in the presence of 0.5 mM diaminodurene (DAD) as fast electron donor to  $\text{P}^+$  (40, 41). In the analysis of charge recombination, nonlinear least-squares minimization was performed by computer routines based on a modified Marquardt algorithm, and confidence intervals of fitting parameters were estimated by an exhaustive search method as described in ref 42.

## RESULTS

**Comparison of the Kinetics of Charge Recombination in RC-Only and in RC–LH1 Complexes.** Figure 1 shows the decay kinetics of  $\text{P}^+$  generated by a laser pulse in RC–LH1 (trace a) and in RC-only (trace b) preparations. Normalization of the traces to the maximal absorbance change immediately after photoexcitation shows evidence that the recovery



Table 1: Kinetic Parameters of  $P^+Q_B^-$  Charge Recombination and Cofactor Stoichiometries in RC–LH1 and RC-Only Preparations<sup>a</sup>

preparation	$\langle k \rangle$ (s <sup>-1</sup> )	$\sigma$ (s <sup>-1</sup> )	$A_f$ (%)	UQ <sub>10</sub> /P <sup>+</sup>	BChl/P <sup>+</sup>
RC–LH1 from photosynthetically grown cells					
prep 1	0.28 (0.25, 0.31)	0.22 (0.19, 0.26)	16.4 (8.4, 22.9)	10.5 ± 0.7	35.0 ± 4.7
prep 2	0.30 (0.28, 0.31)	0.32 (0.30, 0.35)	17.9 (14.3, 22.5)	11.3 ± 0.5	34.0 ± 1.8
RC–LH1 from semiaerobically grown cells					
prep 1	0.21 (0.20, 0.22)	0.21 (0.20, 0.22)	15.9 (11.8, 19.0)	16.2 ± 0.6	23.5 ± 1.9
prep 2	0.21 (0.20, 0.22)	0.20 (0.19, 0.21)	14.6 (11.3, 17.8)	14.3 ± 3.0	27.2 ± 1.2
RC–LH1 from X <sup>-</sup> strain	0.29 (0.28, 0.30)	0.21 (0.19, 0.23)	6.5 (0.8, 11.0)	17.6 ± 1.2	36.9 ± 0.9
RC-only					
prep 1	1.01 (0.97, 1.06)	0.35 (0.28, 0.41)	22.3 (19.3, 25.3)	1.5 ± 0.4	4.5 ± 0.5
prep 2	0.97 (0.95, 1.00)	0.39 (0.36, 0.42)	19.4 (17.5, 21.1)	1.8 ± 0.4	4.0 ± 0.5

<sup>a</sup> Kinetics of charge recombination were measured at 605 nm at 25 °C and fitted to the sum of a power law and an exponential decay with a fixed rate constant equal to 8.2 s<sup>-1</sup> (see eq 1). Values in parentheses give the extremes of the confidence intervals within one standard deviation. See text for further details.

kinetics are drastically slowed in RC–LH1 as compared to RC-only complexes. In both cases the kinetics include two well-separated components and have been fitted to a fast exponential term plus a slowly decaying power law, according to

$$P^+(t)/P^+(0) = A_f \exp(-k_f t) + (1 - A_f)(1 + k_0 t)^{-n} \quad (1)$$

where  $A_f$  represents the fraction of reaction centers (with the  $Q_B$  site empty or damaged during the purification procedure) that recombines from the state  $P^+Q_A^-$  with a typical  $k_f \approx 10$  s<sup>-1</sup> (11). The dominating slow component, attributed to  $P^+Q_B^-$  recombination, deviates slightly but systematically from an exponential behavior also in RC–LH1 preparations, as already reported for RC-only complexes (37). The use of a power law to fit this kinetic phase implies a continuous distribution of rate constants (42, 43). The average rate constant,  $\langle k \rangle$ , and the width,  $\sigma$ , of the rate distribution function are related to the parameters  $k_0$  and  $n$  in eq 1 by  $\langle k \rangle = nk_0$  and  $\sigma^2 = nk_0^2$  (42). When fitting the kinetics to eq 1, we fixed the rate constant  $k_f$  of the fast phase to 8.2 s<sup>-1</sup> as measured for  $P^+Q_A^-$  recombination in suspensions of RC-only deprived of the secondary acceptor  $Q_B$  (42). This was done in order to avoid effects of strong parameter correlation and in view of the relatively poor sampling of the fast kinetic component in traces recorded over several seconds. The validity of such an approach is justified by the fact that, in all preparations examined, leaving  $k_f$  as an adjustable parameter yields values ranging between 8 and 10 s<sup>-1</sup>, without any systematic difference between RC-only and RC–LH1 preparations. In agreement with this observation, when electron transfer to  $Q_B$  is inhibited by *o*-phenanthroline, essentially the same kinetics of  $P^+Q_A^-$  recombination are measured in RC-only and RC–LH1 complexes, characterized by a rate constant  $k \approx 10$  s<sup>-1</sup> at 298 K (see below).

The described fitting procedure yields, in RC–LH1s purified from photosynthetically grown cells, an average rate constant ( $\langle k \rangle = 0.29$  s<sup>-1</sup>) 3.5 times smaller than in RC-only ( $\langle k \rangle = 1.0$  s<sup>-1</sup>). In both cases kinetics are moderately distributed with a comparable width of approximately 0.2–0.4 s<sup>-1</sup>, and the slow phase accounts for approximately 80% of  $P^+$  decay (see Figure 1). This relatively narrow distribution of rate constants agrees with the results of a previous analysis in RC-only (37). Following the procedure exemplified in Figure 1, the kinetics of  $P^+$  decay after a laser pulse have been analyzed in a series of preparations of core complexes

isolated from WT cells grown under photosynthetic conditions and from WT and X<sup>-</sup> strain cells grown under semiaerobic conditions. Fitting parameters for the corresponding kinetics are summarized in Table 1, which also includes two independent RC-only preparations. Drastic slowing down of the kinetic phase attributed to  $P^+Q_B^-$  recombination appears to be a general feature of RC–LH1 core complexes as compared to RC-only. This slowing is, however, significantly more pronounced in WT preparations from semiaerobically grown cells than in complexes purified from photosynthetically grown WT cells. In the former case the slow component of  $P^+$  decay exhibits an average rate constant,  $\langle k \rangle = 0.21$  s<sup>-1</sup>, four times smaller than in RC-only complexes ( $\langle k \rangle = 1.0$  s<sup>-1</sup>). In core complexes purified from the PufX-deleted strain (see Materials and Methods) the  $\langle k \rangle$  value is essentially coincident with that obtained in RC–LH1 from photosynthetically grown WT cells.

To safely attribute the extremely slow  $P^+$  decay observed in core complexes to recombination of the  $P^+Q_B^-$  state, it is important to exclude the occurrence of side redox reactions which, on the time scale of several seconds, could contribute in principle to oxidize the light-generated semiquinone at the  $Q_B$  site, thus inducing slow  $P^+$  rereduction by exogenous electron donors. The stability of the semiquinone formed upon laser excitation at the  $Q_B$  site has been therefore tested in the RC–LH1 complexes by monitoring the laser-induced formation of semiquinone at 446 nm, in the presence of added DAD. This exogenous electron donor completely rereduces the photooxidized  $P^+$  in a few milliseconds, so that the  $PQ_A Q_B^-$  and  $PQ_A^- Q_B$  states are trapped (40, 41). Under these conditions, in RC–LH1 complexes, the flash-generated semiquinone signal decayed by less than 10% over 20 s (not shown). This indicates that flash-induced  $Q_B^-$  is quite stable in core complexes over the time of  $P^+$  decay measured in the absence of exogenous electron donors (Figure 1). Assuming differential extinction coefficients  $\Delta\epsilon_{605} = 19.5$  mM<sup>-1</sup> and  $\Delta\epsilon_{446} = 8.5$  mM<sup>-1</sup> for  $P^+$  and semiquinone, respectively (35, 36, 44), a  $Q^-/P^+$  ratio close to 1 has been estimated, confirming the stability of the quinone acceptor radicals. These measurements unambiguously show that the very slow  $P^+$  decay kinetics observed in LH1–RC complexes reflect a genuine charge recombination process.

The temperature dependence of  $P^+Q_B^-$  recombination kinetics has been examined in LH1–RC complexes purified from photosynthetically grown WT cells over the range 275 K ≤  $T$  ≤ 305 K. Panel A of Figure 2 presents an Arrhenius plot of the average rate constant  $\langle k \rangle$  determined by the above-

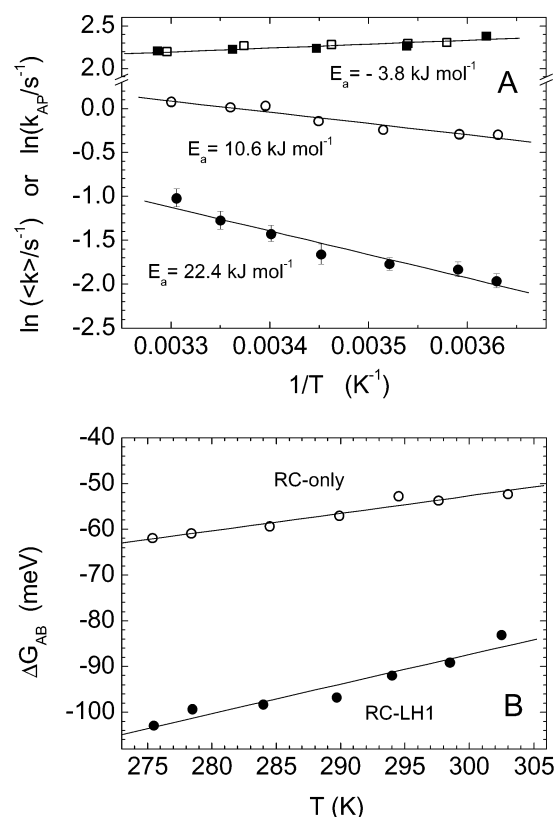


FIGURE 2: Temperature dependence of  $P^+Q_B^-$  (circles) and  $P^+Q_A^-$  (squares) recombination kinetics in RC–LH1 (filled symbols) and RC-only complexes (open symbols). Panel A: Arrhenius plot of the average rate constant  $\langle k \rangle$  of the slow kinetic component of  $P^+$  decay ( $P^+Q_B^-$  recombination) and of the rate constant  $k_{AP}$  measured in the presence of 10 mM *o*-phenanthroline ( $P^+Q_A^-$  recombination). Error bars correspond to confidence intervals within one standard deviation. Panel B: Temperature dependence of the free energy difference  $\Delta G_{AB}$  between the  $P^+Q_AQ_B^-$  and the  $P^+Q_A^-Q_B$  states evaluated from the data of panel A as described in the text. Best fitting straight lines ( $\Delta G_{AB} = \Delta H_{AB} - T\Delta S_{AB}$ ) correspond to  $\Delta H_{AB} = -(281 \pm 23)$  meV and  $\Delta S_{AB} = -(0.65 \pm 0.08)$  meV  $K^{-1}$  for RC–LH1 and  $\Delta H_{AB} = -(167 \pm 12)$  meV and  $\Delta S_{AB} = -(0.38 \pm 0.04)$  meV  $K^{-1}$  for RC-only.

described fitting procedure in core complexes and in a RC-only preparation. A stronger temperature dependence is obtained in the former case, corresponding to an apparent activation energy of approximately 22 kJ mol $^{-1}$  as compared to 11 kJ mol $^{-1}$  in the RC-only complex. The kinetics of  $P^+Q_A^-$  recombination were examined by measuring  $P^+$  decay in the same RC–LH1 and RC-only preparations in the presence of 10 mM *o*-phenanthroline. Fitting the decays to a single exponential yielded very close values of the rate constant  $k_{AP}$  for  $P^+Q_A^-$  recombination in the two systems. Rate constants vary in both preparations between approximately 10.8 s $^{-1}$  at  $T = 275$  K and 9.0 s $^{-1}$  at  $T = 305$  K (see Figure 2A), exhibiting a small, negative, apparent activation energy of approximately  $-3.8$  kJ mol $^{-1}$ . The coincidence of  $k_{AP}$  values and the higher apparent activation energy measured for  $P^+Q_B^-$  recombination in LH1–RC complexes strongly suggest that stabilization of the  $P^+Q_AQ_B^-$  state with respect to the  $P^+Q_A^-Q_B$  is increased in the presence of the LH1 antenna (see Discussion).

**Ubiquinone Complement and Antenna Size in Core Complexes.** As analyzed in detail by Shinkarev and Wraight (45), the kinetics of  $P^+Q_AQ_B^-$  recombination can be considerably affected by the binding equilibrium of ubiquinone

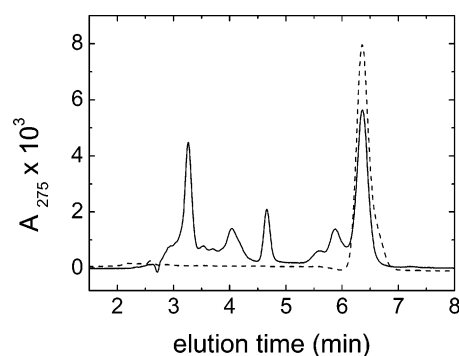


FIGURE 3: HPLC chromatograms of the extract from a RC–LH1 preparation (prep 1 from photosynthetically grown cells in Table 1) (continuous line) and of a standard solution of UQ $_{10}$  corresponding to 150 pmol (dashed line). The injected extract of the core complexes corresponds to 6.7 pmol of photooxidizable reaction center.

at the  $Q_B$  site when this process occurs rapidly over the time scale of  $P^+Q_A^-$  recombination. Recent investigations performed on RC-only complexes in inverted micelles (27) as well as in artificial lipid vesicles (25) are indeed consistent with a fast quinone exchange at the  $Q_B$  site and indicate that the observed rate constant of  $P^+Q_AQ_B^-$  recombination is sensitive to the concentration of quinone  $[Q]$  in rapid equilibrium with the binding site (i.e., it decreases at increasing  $[Q]$ ; see Discussion). This view clearly prompts for a determination of the quinone complement associated with the purified core complexes in which a marked slowing down of the recombination kinetics was observed.

The ubiquinone content of the examined core complex and RC-only preparations was determined by exhaustive extraction and HPLC analysis (see Materials and Methods). Figure 3 shows the chromatogram of a pure ubiquinone-10 sample (dashed line) overlaid to a typical chromatogram of a RC–LH1 extract (continuous line). Spectral analysis of the eluates has confirmed the attribution to oxidized UQ $_{10}$  of the peak at 6.4 min and has indicated that the components eluted at shorter times are mainly carotenoids. This analysis indicates also that the carotenoid contamination of the UQ $_{10}$  fraction is lower than 10%. In parallel measurements the total photooxidizable primary donor  $P$  was estimated by measuring the absorbance change induced at 605 and 542 nm (35, 36) by trains of actinic xenon flashes. In the case of purified RC-only preparations, excitation by continuous light was used to achieve saturation (see Materials and Methods). The stoichiometric ratios UQ $_{10}/P^+$  obtained on this basis are summarized in Table 1, which also includes the corresponding bacteriochlorophyll to  $P^+$  ratios (BChl/ $P^+$ ). As expected, determination of this stoichiometry in RC-only preparations yielded a value consistent with 4 BChl per RC, while a number of ubiquinone molecules per RC close to 2 was found, in agreement with previous measurements (46, 47). In RC–LH1 core complexes purified from semiaerobically grown WT cells an average ratio of 25 BChl molecules per complex was obtained, in reasonable agreement with recent low-resolution structural data which suggest the presence of 12  $\alpha\beta$  heterodimers per LH1 ring (9). The BChl/ $P^+$  ratio increases to approximately 37 in core complexes purified from the PufX-deleted strain, a value consistent with previous observations (6, 7) and with the notion that a closed ring of  $\alpha\beta$  heterodimers surrounds the RC in the absence of the PufX protein. In RC–LH1 complexes purified from photosyntheti-

Table 2: Bacteriochlorophyll and Ubiquinone-10 to P<sup>+</sup> Stoichiometries Determined in Different Fractions during the Purification of Core Complexes<sup>a</sup>

sample	BChl/P <sup>+</sup>	UQ <sub>10</sub> /P <sup>+</sup>
chromatophores	142 ± 8	25 ± 5
NaBr-washed chromatophores	175 ± 10	38 ± 3
supernatant	173 ± 7	30 ± 5
pellet	53 ± 6	43 ± 2

<sup>a</sup> See text for details.

cally grown WT cells the number of BChl molecules per P<sup>+</sup> is close to 35, i.e., systematically and significantly larger than in complexes purified from semiaerobically grown bacteria.

Surprisingly, in all of the core complex preparations examined a large pool of ubiquinone-10 is detected; in fact, the stoichiometry UQ<sub>10</sub>/P<sup>+</sup> ranges from approximately 10 to 15 in RC–LH1 from photosynthetically and semiaerobically grown WT cells, respectively. An even larger pool (18 UQ<sub>10</sub> molecules per photooxidizable RC) was determined in core complexes isolated from the X<sup>−</sup> strain. The large ubiquinone complements associated with RC–LH1 represent a considerable fraction of the total ubiquinone present in the membrane phase. RC–LH1 complexes, exhibiting a UQ<sub>10</sub>/P<sup>+</sup> ratio close to 11, were isolated from chromatophores characterized by a stoichiometry of 25 ubiquinone molecules per photooxidizable RC.

The high UQ<sub>10</sub>/P<sup>+</sup> ratio found in RC–LH1 fractions is unlikely to be due to ubiquinone solubilized in a pure detergent phase. Analysis of the different fractions collected over the whole sucrose gradient used to separate photosynthetic membrane complexes (not shown) has revealed sizable amounts of UQ<sub>10</sub> in the top fraction of the gradient, where low-density detergent micelles are expected to be layered. To further examine the possibility that the large ubiquinone content of isolated core complexes is simply due to a strong preferential portion of UQ<sub>10</sub> in the detergents with respect to the membrane phospholipids, we have determined the UQ<sub>10</sub>/P<sup>+</sup> ratio in different fractions during the purification procedure. As shown in Table 2, chromatophores washed with 2 M NaBr are characterized by an enrichment in the number of both BChl and UQ<sub>10</sub> per P<sup>+</sup>, presumably due to inactivation of photochemistry in a fraction of RCs. Subsequent steps include detergent extraction with OG and sodium cholate and ultracentrifugation (see Materials and Methods). The BChl/P<sup>+</sup> and UQ<sub>10</sub>/P<sup>+</sup> stoichiometries have been determined in the pellet and in the supernatant which is charged on the 10–40% sucrose gradient for the isolation of the LH2 and RC–LH1 complexes. The number of BChl per photoactive reaction center is essentially unaffected in the supernatant and drastically reduced in the residual pellet, indicating a good yield of detergent extraction of the photosynthetic complexes. The UQ<sub>10</sub>/P<sup>+</sup> ratio decreases from 38 in the washed membrane fraction to 30 in the supernatant. At variance, a sizable increase of the UQ<sub>10</sub>/P<sup>+</sup> stoichiometry is observed in the residual membrane pellet. These observations argue against a segregation of quinones in the detergent phase.

The concentration of the LH2 complexes purified on the same sucrose gradient from which the LH1–RCs were isolated has been evaluated from the total BChl content by assuming 27 BChl molecules per complex (39). On this basis,

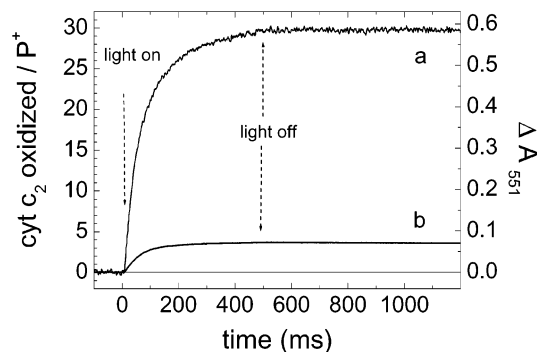


FIGURE 4: Cytochrome *c*<sub>2</sub> oxidation, measured at 551 nm, induced by continuous photoexcitation of RC–LH1 from photosynthetically grown WT cells (prep 2 in Table 1) (curve a) and of RC-only complexes (prep 1 in Table 1) (curve b). The P<sup>+</sup> concentration in the assays was 0.067 and 2.77 μM in RC–LH1 and RC-only samples, respectively. Both signals have been normalized to a P<sup>+</sup> concentration equal to 1 μM. Purified cyt *c*<sub>2</sub> was added at 50 and 10 times excess concentration over the photoactive RC in the RC–LH1 and RC-only samples, respectively. The left scale gives the number of cyt *c*<sub>2</sub> oxidized per reaction center.

determination of ubiquinone in the LH2 fraction yields approximately 1.4 UQ<sub>10</sub> molecules per LH2, well below the values obtained in RC–LH1. Since both LH2 and RC–LH1 fractions come from the same detergent extract, this observation again indicates that the high UQ<sub>10</sub> content of the RC–LH1 is not simply due to partition of ubiquinone in the detergents but is a peculiar feature of the core complexes.

To confirm the analytical determinations of the ubiquinone to RC stoichiometries and to assess the functionality of the detected quinone molecules in accepting electrons at the Q<sub>B</sub> site, we used an alternative quinone assay based on the rapid oxidation of cytochrome *c*<sub>2</sub> by the RC under continuous illumination (47). In the presence of excess reduced cyt *c*<sub>2</sub> the number of turnovers which the RC can sustain under continuous light is limited by the number of oxidized ubiquinone molecules available as electron acceptors at the Q<sub>B</sub> site. More precisely, when *n* ubiquinone molecules per RC are present in addition to the primary acceptor Q<sub>A</sub>, (2*n* + 1) molecules of cyt *c*<sub>2</sub> per RC are expected to be oxidized under continuous illumination. Figure 4 shows the oxidation of exogenously added cyt *c*<sub>2</sub> (monitored at 551 nm) by RC–LH1 and RC-only complexes exposed for 500 ms to continuous light excitation. Traces have been normalized on the basis of the total concentration of photooxidizable donor P present in the respective samples, and a differential extinction coefficient Δε = 19.5 mM<sup>−1</sup> cm<sup>−1</sup> at 551 nm has been used to evaluate the concentration of oxidized cyt *c*<sub>2</sub> (35). This can be measured from the plateau reached by the cyt *c*<sub>2</sub> oxidation trace, since oxidized cyt *c*<sub>2</sub> is stable on the time scale of the measurement. From the data in Figure 4, total UQ<sub>10</sub>/P<sup>+</sup> ratios of 14 and 1.5 can be evaluated in the case of RC–LH1 and RC-only, respectively. These values compare well with the stoichiometries evaluated by HPLC that gave 11 and 1.5 UQ<sub>10</sub>/RC, respectively. It appears, therefore, that the large ubiquinone pool analytically detected in RC–LH1 preparations is fully available to the Q<sub>B</sub> site as electron acceptor.

## DISCUSSION

*A Ubiquinone Pool Copurifies with RC–LH1 Core Complexes.* Our determinations of the BChl content of core



complexes purified from the semiaerobically grown WT and the PufX-deleted strains are in reasonable agreement with previous estimates and with the structural information available for RC–LH1 complexes in *Rb. sphaeroides* and in related species. When subtracting from the stoichiometric ratios of Table 1 the four BChl molecules belonging to the RC, it appears that deletion of PufX leads to an increase in the number of BChl molecules per LH1 from  $22 \pm 2$  to  $33 \pm 1$ , i.e., to a change in the number of  $\alpha\beta$  heterodimers forming the LH1 ring from approximately 11 to 16. A number of 12  $\alpha\beta$  heterodimers has been proposed for the PufX–LH1 complex on the basis of low-resolution structural data obtained in vivo (8) and in purified complexes (9). From previous determinations of BChl content in the purified complexes, stoichiometries of  $13 \pm 2$  and  $18 \pm 3$   $\alpha\beta$  heterodimers per LH1 complex can be evaluated for the WT and the PufX-deleted strain, respectively (7). Estimates of the size of the LH1 antenna in chromatophores from green LH2-deleted strains of *Rb. sphaeroides* yielded values of  $23.6 \pm 1.8$  and  $34.9 \pm 1.8$  BChl per complex in the presence and in the absence of the PufX protein, respectively (6).

When comparing core complexes purified from semiaerobically grown with those from photosynthetically grown WT cells, we observed in the latter systematically larger BChl/ $P^+$  ratios which suggest an increase of the LH1 antenna size from  $22 \pm 2$  to  $30 \pm 4$ . Interestingly, the crystallographic structure of the core complex purified from photosynthetically grown cells of the related species *Rps. palustris* shows 15  $\alpha\beta$  heterodimers, consistent with a stoichiometry of 30 BChl per LH1 (23).

In membrane from *Rb. sphaeroides* and *Rhodobacter capsulatus* ubiquinone-10 is present in large stoichiometric excess over the RC. The size of this (thermodynamically homogeneous) pool varies from approximately 20 to 60  $UQ_{10}$  molecules per RC depending on the growth conditions (see, e.g., refs 33, 48, and 49). Its role in mediating the cyclic electron transfer catalyzed by the RC and the  $bc_1$  complex is well established and explained by the current Q-cycle schemes (12). A number of studies performed in chromatophore vesicles and exploiting different approaches are consistent with the notion of a diffusional pathway for  $UQH_2/UQ$  between the RC and the  $bc_1$  complex. These investigations indicate that oxidation of  $UQH_2$  at the  $Q_o$  site of the  $bc_1$  complex involves a collisional reaction, that the oxidizing site is in rapid equilibrium with a large ubiquinone pool, and that ubiquinone, as well as soluble cyt  $c_2$ , diffuses between reaction sites in a domain which includes several electron transfer chains and which seems to coincide with the chromatophore vesicle (12, 33, 50–52). On the other hand, studies with intact cells have led to a proposal that the enzymes of the photosynthetic electron transfer chain are organized in supercomplexes and that cofactor diffusion between reaction sites occurs in vivo in restricted domains limited to a small number of interacting complexes (53–56). Data interpreted as evidence for the existence of a heterogeneous spatial distribution of ubiquinone within the chromatophore membrane under oxidizing conditions have been put forward by Drachev et al. (57). These different views are currently debated, and several aspects of the in vivo interaction of quinone from the pool with its reaction partners remain open to investigation (see, e.g., refs 58–61).

In the present paper we show that, when relatively mild detergent extraction conditions are used to isolate RC–LH1 complexes, the purified core complex fractions contain a large complement of ubiquinone molecules. Analytical ubiquinone determinations yield  $UQ_{10}/RC$  ratios of approximately 10 in core complexes purified from photosynthetically grown WT cells. This stoichiometry corresponds to 40% of the total ubiquinone content of intact membrane vesicles ( $25 UQ_{10}/RC$ ). A comparable, large stoichiometry is obtained when the quinone is evaluated by a functional assay based on the number of cyt  $c_2$  molecules per RC rapidly oxidized under continuous illuminations. This demonstrates that all of the ubiquinone molecules analytically detected in the purified RC–LH1 fractions are promptly available as electron acceptors at the  $Q_B$  site. More than 80% of the maximal cyt  $c_2$  oxidation level is reached in the first 100 ms of continuous photoexcitation, giving a lower limit for the rate of quinone exchange at the  $Q_B$  site. Even higher  $UQ_{10}/RC$  ratios have been determined in core complexes purified from semiaerobically grown WT and  $X^-$  cells (see Table 1).

Several independent lines of evidence show that the high  $UQ_{10}/RC$  ratios detected in the purified RC–LH1 preparations are not due to quinone artifactually segregated into the detergent phase during extraction: (a)  $UQ_{10}$  containing detergent micelles are layered on top of the sucrose gradient over which RC–LH1 and LH2 complexes are separated; (b) the  $UQ_{10}/P^+$  ratio determined in the residual membrane pellet during the purification procedure is higher than that of the detergent extract (supernatant), suggesting that ubiquinone extraction by detergent is less efficient than RC–LH1 extraction (see Table 2); (c) the ubiquinone concentration in the LH2 fraction (corresponding to 1.4  $UQ_{10}$  molecules per LH2) is much lower than in the RC–LH1 fraction coming from the same detergent extract; (d)  $UQ_{10}$  is expected to exchange slowly between RC–LH1 micelles and pure detergent micelles (26) so that  $UQ_{10}$  molecules in pure detergent micelles disconnected from the RC–LH1 complex would not be available as electron acceptors at the  $Q_B$  site as required for the fast multiple oxidation of cytochrome  $c_2$  observed under continuous illumination. We conclude, therefore, that the whole  $UQ_{10}$  complement detected in RC–LH1 fractions is strictly associated with the core complexes.

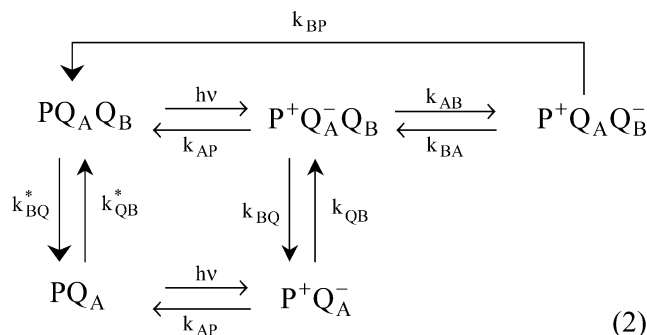
In light of the limited information available on detergent–RC interaction (62–64) it is conceivable that, also in the case of the RC–LH1 and LH2 complexes, detergents fill the available space around the membrane-spanning helices, providing an hydrophobic phase for  $UQ_{10}$ . This phase is likely to include tightly bound lipids, as recently evidenced for RC-only complexes (65–67). Assuming that the  $UQ_{10}$  is aspecifically distributed in this hydrophobic belt both in RC–LH1 and in LH2, in the absence of other interactions, the number of  $UQ_{10}$  molecules per RC–LH1 and LH2 is expected to be roughly proportional to the diameter of the respective ring structures. In this hypothesis, diameters from 90 (4) to 110 Å (9) for the RC–LH1 (thought of as a monomer) and of 70 (4) Å for the LH2 would correspond to a ratio of the  $UQ_{10}/complex$  ranging from 1.3 to 1.6 times larger in RC–LH1 as compared to LH2. This is likely to be an upper limit, since the empty LH2 ring, although smaller, could locate in its inner space lipid and/or detergent molecules, providing a more extended hydrophobic phase

for quinone solubilization. At variance, from the data of Table 1 it appears that the stoichiometry of the  $UQ_{10}/\text{complex}$  is always at least 6 times larger in RC–LH1 than in LH2. These considerations strongly suggest that the large ubiquinone pool copurifying with the RC–LH1 is the result of specific interactions of the cofactor with the core complex, which in vivo are presumed to determine an heterogeneity in the spatial distribution of ubiquinone.

The structure of the core complex suggests the space between RC and LH1 as a putative location for hydrophobic guest molecules. From the low-resolution projection map of the complex (9) the area between the LH1 ring and the RC, roughly evaluated as the area between two concentric circles of diameter  $\sim 75$  and  $\sim 50$  Å, can be estimated as  $\sim 2500$  Å<sup>2</sup>. When assuming a thickness of about 30 Å for the hydrophobic domain, this translates into a volume of about  $7.5 \times 10^4$  Å<sup>3</sup>. On the basis of a  $UQ_{10}$  molar volume of approximately  $1070$  cm<sup>3</sup> mol<sup>−1</sup> [estimated from the density of a  $UQ_{10}$  solution in hexane (G. Palazzo, unpublished data)], a total complement of 10–15  $UQ_{10}$  molecules per RC–LH1 complex would correspond to a volume of  $(1.8–2.7) \times 10^4$  Å<sup>3</sup>. Although the conformation of the  $UQ_{10}$  molecules copurifying with the complex (and consequently their actual volume) is not known, the above estimates suggest that the space between the antenna and the RC can well accommodate the ubiquinone complement.

**Stabilization of the  $P^+Q_AQ_B^-$  State in RC–LH1 Complexes.** Despite the wide literature on the kinetics of charge recombination events measured in RC-only and the increasing structural knowledge of RC–LH1 complexes of photosynthetic bacteria, the effect of the antenna system on these intraprotein electron transfer processes has not yet been studied. In the present paper we have compared the recombination kinetics of the light-induced  $P^+Q_A^-Q_B$  and  $P^+Q_AQ_B^-$  states in detergent suspensions of RC–LH1 core and RC-only complexes purified from *Rb. sphaeroides*. In the presence of *o*-phenanthroline, essentially the same  $P^+Q_A^-Q_B$  recombination kinetics is observed following a light pulse in these two systems (see Figure 2A). At variance, in the absence of the inhibitor, the recombination kinetics of the flash-generated  $P^+Q_AQ_B^-$  state is strongly slowed in the presence of the LH1 antenna (see Figures 1 and 2 and Table 1). The average rate constant characterizing  $P^+Q_AQ_B^-$  recombination decreases from approximately  $1$  s<sup>−1</sup> in RC-only to 0.3 in RC–LH1 complexes isolated from photosynthetically grown WT cells; the slowing effect appears more pronounced ( $\langle k \rangle = 0.2$  s<sup>−1</sup>) in core complexes purified from semiaerobically grown WT cells, while a  $\langle k \rangle$  value close to  $0.3$  s<sup>−1</sup> has been measured in RC–LH1 from the PufX-deleted strain. Recombination appears therefore three to four times slowed in all core complexes, being also possibly modulated by different structural organizations of the RC–LH1 complex, as suggested by the different BChl/ $P^+$  ratios measured in core complexes obtained from differently grown cells or X<sup>−</sup> strain.

Possible pathways and mechanisms of charge recombination in RCs have been thoroughly discussed by Shinkarev and Wraight (45) on the basis of the following general scheme shown in eq 2 in which both a direct (rate constant  $k_{BP}$ ) and an indirect recombination route (by thermal repopulation of  $P^+Q_A^-Q_B$ ) are taken into account and the binding of quinone at the  $Q_B$  site is explicitly considered.



The rate constants  $k_{AP}$ ,  $k_{AB}$ ,  $k_{BA}$ ,  $k_{BQ}$ , and  $k_{BQ}^*$  are true first-order rate constants, while  $k_{QB}$  and  $k_{QB}^*$  are the pseudo-first-order binding rate constants of pool quinones to the  $Q_B$  site, i.e.,  $k_{QB} = k_{QB}'[Q]$  and  $k_{QB}^* = k_{QB}^*[Q]$ , with  $[Q]$  being the ubiquinone concentration. Kleinfeld et al. (19) have demonstrated that in RC-only complexes recombination of the  $P^+Q_AQ_B^-$  proceeds essentially via  $P^+Q_A^-Q_B$ , with the contribution of the direct route being negligible. The direct pathway has been characterized in RC-only complexes in which the primary acceptor,  $Q_A$ , has been replaced with low potential quinones, raising the energy level of the state  $P^+Q_A^-Q_B$  relative to  $P^+Q_AQ_B^-$  and thus disfavoring the indirect pathway. Schmid and Labahn (68) have determined a  $k_{BP}$  value of  $0.12$  s<sup>−1</sup> at  $T = 293$  K,  $6 < \text{pH} < 8$ , in the presence of 60% glycerol. In the absence of cryosolvents  $k_{BP} \approx 0.19$  s<sup>−1</sup> has been evaluated under similar conditions (69). In view of these values, the direct recombination route cannot be disregarded a priori when analyzing  $P^+Q_AQ_B^-$  recombination in core complexes; in the presence of the LH1 antenna, in fact, the recombination kinetics is characterized by an observable average rate constant ( $\langle k \rangle \approx 0.2–0.3$  s<sup>−1</sup>) of the same order of magnitude of  $k_{BP}$  in RC-only complexes. Shinkarev and Wraight (45) have shown that the scheme in eq 2 can be analytically solved under two assumptions, which appear quite reasonable in the case of both RC-only and RC–LH1 complexes; i.e., (a) electron transfer between  $Q_A$  and  $Q_B$  is much faster than all other reactions of the scheme in eq 2, so that quasi-equilibrium can be assumed between states  $P^+Q_AQ_B^-$  and  $P^+Q_A^-Q_B$  (12, 13, 19); (b) pool quinone exchanges rapidly at the  $Q_B$  site, so that one can assume quasi-equilibrium between states  $P^+Q_A^-Q_B$  and  $P^+Q_A^-$  (25–27). Under these conditions the observed rate constant of charge recombination is given by

$$k \approx \left( k_{AP} + k_{BP} L_{AB} \frac{K}{1 + K} \right) / \left( 1 + L_{AB} \frac{K}{1 + K} \right) \quad (3)$$

where  $L_{AB} = k_{AB}/k_{BA}$  is the equilibrium constant for electron transfer from  $Q_A$  to  $Q_B$  and  $K = k_{QB}'[Q]/k_{BQ}$  is the dimensionless equilibrium constant of quinone binding to the  $Q_B$  site in the  $P^+Q_A^-$  state.

We found that a large, functional ubiquinone pool copurifies with RC–LH1 complexes, resulting in  $UQ_{10}/P^+$  ratios at least 5 times larger than in RC-only. A first question we can address by using eq 3 is whether and to which extent a higher quinone concentration can account for the slower recombination kinetics observed in core complexes. By considering  $dk/dK$ , it is easily seen that eq 3 predicts indeed a decrease in the rate constant  $k$  upon increasing  $[Q]$  (i.e.,  $K$ ), when  $k_{BP} < k_{AP}$ . The rate constant  $k_{AP}$  is close to  $10$  s<sup>−1</sup>



Table 3: Thermodynamic Parameters for the Electron Transfer between  $Q_A$  and  $Q_B$  Evaluated for Different Environments of the RC<sup>a</sup>

system	$\Delta G_{AB}$ (meV)	$\Delta H_{AB}$ (meV)	$\Delta S_{AB}$ (meV K <sup>-1</sup> )	ref
RC in OG/cholate	−(56 ± 2)	−(167 ± 12)	−(0.38 ± 0.04)	this work
RC–LH1 in OG/cholate	−(91 ± 3)	−(281 ± 23)	−(0.65 ± 0.08)	this work
RC in LDAO	−(71.4 ± 1.4)	−(150 ± 11)	−(0.27 ± 0.03)	24
RC in LDAO	−69	−230	−0.55	19
RC in LDAO	−78.5 <sup>b</sup>			26
RC in reverse micelles	−(81 ± 3)	−(140 ± 7)	−(0.20 ± 0.03)	27
RC in lipid vesicles	−(81 ± 0.5)	−(157 ± 12)	−(0.26 ± 0.04)	25
chromatophores	−120 <sup>c</sup>			20

<sup>a</sup> Unless otherwise stated, values of the free energy changes ( $\Delta G_{AB}$ ) are given at 293 K. <sup>b</sup> Evaluated at 295 K. <sup>c</sup> Evaluated at 309 K.

both in RC-only and in RC–LH1 complexes and  $k_{BP} < 0.2$  s<sup>-1</sup> (68, 69) in RC-only. In RC–LH1  $k_{BP}$  cannot be larger than the observed  $\langle k \rangle$  (ranging from 0.2 to 0.3 s<sup>-1</sup>) so that the inequality  $k_{BP} < k_{AP}$  will certainly hold also in core complexes. It appears, therefore, that according to eq 3 an increase in the quinone concentration associated with the RC could in principle slow P<sup>+</sup>Q<sub>A</sub>Q<sub>B</sub><sup>-</sup> recombination. However, the strong slowing down of charge recombination observed in core complexes cannot be solely due to a quinone effect, as will be shown in the following on the basis of eq 3 and of kinetic data available for RC-only complexes.

Under saturating quinone concentration, i.e., for  $[Q] \rightarrow \infty$ , the observed rate  $k$  will approach a minimal value,  $k_{min}$ , given by

$$k_{min} = (k_{AP} + k_{BP}L_{AB})/(1 + L_{AB}) \quad (4)$$

The equilibrium constant  $L_{AB}$  has been measured by a number of laboratories obtaining at room temperature values which range from 14 to 22 in LDAO suspensions of RCs (19, 24, 26). A value of 22 has been obtained for RC incorporated in artificial phospholipid vesicles (25) and in reverse micelles of phospholipids in *n*-hexane (27). Since  $k_{AP} \approx 10$  s<sup>-1</sup> in RC-only and in RC–LH1, and  $k_{BP}$  values range between 0.12 s<sup>-1</sup> and 0.19 s<sup>-1</sup>, eq 4 yields  $k_{min}$  values between 0.84 and 0.55 s<sup>-1</sup>. It appears, therefore, that an increase in the quinone concentration can at most decrease the observed rate constant  $k$  by less than a factor of 2, being unable to account for the stronger slowing down of the recombination kinetics observed in core complexes ( $\langle k \rangle = 0.2$  s<sup>-1</sup>). We note that, of course, the value of  $k_{min}$  given by eq 4 represents the minimum value of  $k$  attainable also when maximizing the quinone occupancy of the  $Q_B$  site (i.e.,  $K$ ) by changing the rate constants  $k_{BQ}$  and  $k_{QB}'$ . Inspection of eq 4 shows therefore that, to decrease  $k_{min}$ , we are left with only two possibilities, i.e., an increase of  $L_{AB}$  and/or a decrease of  $k_{BP}$ . Indeed, these two effects are clearly related from an energetic point of view. In fact, since  $k_{AP}$  assumes the same value in RC-only and RC–LH1 complexes, the energy level of the state P<sup>+</sup>Q<sub>A</sub><sup>-</sup>Q<sub>B</sub> relative to the ground state is not expected to change in the two systems, and an increase of  $L_{AB}$  implies a stabilization of the state P<sup>+</sup>Q<sub>A</sub>Q<sub>B</sub><sup>-</sup>, i.e., a decrease of its energy level relative to the ground state. This in turn corresponds to a decrease in the free energy drop which drives the direct charge recombination process, so that a decrease in  $k_{BP}$  is also expected (assuming that the reorganization energy of this process is not altered). We conclude therefore that, independently of the actual relative contribution of the direct and of the indirect recombination pathways to  $\langle k \rangle$ , the slowing down of charge recombination

observed in the presence of the LH1 antenna implies necessarily a stabilization of the P<sup>+</sup>Q<sub>A</sub>Q<sub>B</sub><sup>-</sup> state.

The comparison of the temperature dependence of  $\langle k \rangle$  in RC-only and in RC–LH1 complexes (Figure 2A) confirms this conclusion and allows a rough estimate of the enthalpy and entropy changes coupled to Q<sub>A</sub><sup>-</sup> to Q<sub>B</sub> electron transfer in the two systems. A lower limit for the free energy difference ( $-\Delta G_{AB}$ ) between the states P<sup>+</sup>Q<sub>A</sub><sup>-</sup>Q<sub>B</sub> and P<sup>+</sup>Q<sub>A</sub>Q<sub>B</sub><sup>-</sup> can be obtained by assuming saturation of the quinone binding at Q<sub>B</sub> (i.e.,  $K \gg 1$  in eq 3) and disregarding the contribution of the direct route to the observed rate constant  $k$  of P<sup>+</sup>Q<sub>A</sub>Q<sub>B</sub><sup>-</sup> recombination. The limits of the latter assumption, which has been proved correct within a 5% accuracy in RC-only (19), will be discussed a posteriori in the case of core complexes, on the basis of the evaluated ( $-\Delta G_{AB}$ ). Under these conditions, eq 3 reduces to  $k = k_{AP}/(1 + L_{AB})$  and since  $L_{AB} = \exp(-\Delta G_{AB}/k_B T)$ , the free energy change is simply given by

$$\Delta G_{AB} = -k_B T \ln \left( \frac{k_{AP}}{k} - 1 \right) \quad (5)$$

where  $k_B$  is the Boltzmann constant and  $T$  is the absolute temperature (see also ref 19).

Panel B of Figure 2 shows the temperature dependence of  $\Delta G_{AB}$  in RC-only and in RC–LH1 obtained by eq 5 from the respective  $\langle k \rangle$  values (circles in Figure 2A) and by interpolation of the temperature dependence of  $k_{AP}$  measured in the presence of the inhibitor *o*-phenanthroline (squares in Figure 2A). Values of the enthalpy ( $\Delta H_{AB}$ ) and entropy ( $\Delta S_{AB}$ ) changes obtained from Figure 2B are summarized in Table 3. For the sake of comparison, Table 3 also collects previous estimates of the thermodynamic parameters characterizing the electron transfer equilibrium between Q<sub>A</sub> and Q<sub>B</sub> in different environments of the RC. In the case of RC-only, the data of Figure 2B yield  $\Delta H_{AB} = -(167 \pm 12)$  meV and  $\Delta S_{AB} = -(0.38 \pm 0.04)$  meV K<sup>-1</sup>, in good agreement with previous determinations in LDAO suspensions of RCs (24). Comparable values have been reported for RCs in reverse micelles (27) and in lipid vesicles (25) (see Table 3). This results in  $\Delta G_{AB} = -56$  meV at  $T = 293$  K, in good agreement with the values of Kleinfeld et al. (19). In core complexes at  $T = 293$  K,  $-\Delta G_{AB}$  increases to 91 meV (see Figure 2B). The temperature dependence indicates that this considerable stabilization of the state P<sup>+</sup>Q<sub>A</sub>Q<sub>B</sub><sup>-</sup> (35 meV at 293 K) is driven by an almost doubled enthalpic contribution (opposed by an entropy term that is almost twice that measured in RC-only).

To assess the limits of this estimate of  $\Delta G_{AB}$  (in which we neglected the contribution of the direct recombination

route), we can now calculate the corresponding value for  $k_{BP}$  expected for  $\Delta G_{AB} = -91$  meV at 293 K. Since a decrease in the energy level of the state  $P^+Q_AQ_B^-$  relative to the ground state by 35 meV implies the same decrease in the free energy drop ( $-\Delta G_{BP}$ ) driving the direct charge recombination, on the basis of the free energy dependence of  $k_{BP}$  determined by Schmid and Labahn in RC-only complexes (68) a decreased rate constant,  $k_{BP} \cong 0.07$  s<sup>-1</sup>, can be calculated for core complexes. The maximal relative contribution of the direct route to the observed  $\langle k \rangle$  ( $k_{BP}/\langle k \rangle \cong 0.07/0.2$ ) does not exceed 35%. Therefore, although the direct recombination pathway is likely to contribute to  $\langle k \rangle$ , the indirect route will still dominate, and the values of Figure 2B should yield a reasonable estimate of the minimal extent of  $P^+Q_AQ_B^-$  stabilization in RC-LH1.

Quite interestingly in intact chromatophores of *Rb. sphaeroides* the standard free energy decrease accompanying the electron transfer from  $Q_A$  to  $Q_B$  has been estimated as 100 and 120 meV on the basis of the decay rate constant of  $P^+$  and of the intensity of delayed fluorescence, respectively (20). These values are in full agreement with a lower limit of 91 meV, estimated by us in RC-LH1 (see Table 3). It appears, therefore, that the increased stability of the  $P^+Q_AQ_B^-$  state in the native membrane, relative to isolated RC-only complexes, is essentially due to the presence of the LH1 antenna.

In conclusion, the present investigation shows that the RC-LH1 structure is characterized by a specific propensity to retain a large ubiquinone pool and by a considerable decrease in the energy level of the  $P^+Q_AQ_B^-$ . A possible physiological relevance of these effects resides in the fact that both concur in stabilizing the charge-separated state of the RC. We propose therefore that, besides its major light-harvesting function, the LH1 complex plays a role in optimizing in vivo the yield of secondary charge separation.

## ACKNOWLEDGMENT

The authors thank Prof. Dieter Oesterhelt (Max-Planck-Institut für Biochemie, Martinsried) for kindly providing the PufX-deleted strain of *Rb. sphaeroides* and Prof. Romana Fato and Dr. Cristina Pagnucco (University of Bologna) for assistance in HPLC analysis. Dr. Daniel Lévy (Institut Curie, Paris) is kindly acknowledged for critically reading the manuscript.

## REFERENCES

- Hu, X., Damianovic, A., Ritz, T., and Schulten, K. (1998) Architecture and mechanism of the light-harvesting apparatus of purple bacteria, *Proc. Natl. Acad. Sci. U.S.A.* 95, 5935–5941.
- Sundström, V., Pullerits, T., and van Grondelle, R. (1999) Photosynthetic light-harvesting: reconciling dynamics and structure of purple bacterial LH2 reveals function of photosynthetic unit, *J. Phys. Chem. B* 103, 2327–2346.
- Isaacs, N. W., Cogdell, R. J., Freer, A. A., and Prince, S. M. (1995) Light-harvesting mechanisms in purple photosynthetic bacteria, *Curr. Opin. Struct. Biol.* 5, 794–797.
- Walz, T., Jamieson, S. J., Bowers, C. M., Bullough, P. A., and Hunter, C. N. (1998) Projection structures of three photosynthetic complexes from *Rhodobacter sphaeroides*: LH2 at 6 Å, LH1 and RC-LH1 at 25 Å, *J. Mol. Biol.* 282, 833–845.
- Farchaus, J. W., Barz, W. P., Grünberg, H., and Oesterhelt, D. (1992) Studies on the expression of the PufX polypeptide and its requirement for phototrophic growth in *Rhodobacter sphaeroides*, *EMBO J.* 11, 2779–2788.
- McGlynn, P., Hunter, C. N., and Jones, M. R. (1994) The *Rhodobacter sphaeroides* PufX protein is not required for photosynthetic competence in the absence of a light harvesting system, *FEBS Lett.* 349, 349–353.
- Francia, F., Wang, J., Venturoli, G., Melandri, B. A., Barz, W. P., and Oesterhelt, D. (1999) The reaction center-LH1 antenna complex of *Rhodobacter sphaeroides* contains one PufX molecule which is involved in dimerization of this complex, *Biochemistry* 38, 6834–6845.
- Jungas, C., Ranck, J. L., Rigaud, J. L., Joliet, P., and Vermeglio, A. (1999) Supramolecular organization of the photosynthetic apparatus of *Rhodobacter sphaeroides*, *EMBO J.* 18, 534–542.
- Scheuring, S., Francia, F., Busselez, J., Melandri, B. A., Rigaud, J. L., and Levy, D. (2004) Structural role of PufX in the dimerization of the photosynthetic core complex of *Rhodobacter sphaeroides*, *J. Biol. Chem.* 279, 3620–3626.
- Siebert, C. A., Qian, P., Fotiadis, G., Engel, A., Hunter, C. N., and Bullough, P. A. (2004) Molecular architecture of photosynthetic membranes in *Rhodobacter sphaeroides*: the role of PufX, *EMBO J.* 23, 690–700.
- Feher, G., Allen, J. P., Okamura, M. Y., and Rees, D. C. (1989) Structure and function of bacterial photosynthetic reaction centres, *Nature* 339, 111–116.
- Crofts, A. R., and Wraight, C. A. (1983) The electrochemical domain of photosynthesis, *Biochim. Biophys. Acta* 726, 149–185.
- Okamura, M. Y., Paddock, M. L., Graige, M. S., and Feher, G. (2000) Proton and electron transfer in bacterial reaction centers, *Biochim. Biophys. Acta* 1458, 148–163.
- Allen, J. P., Feher, G., Yeates, T. O., Rees, D. C., Deisenhofer, J., Michel, H., and Huber, R. (1986) Structural homology of reaction centers from *Rhodospseudomonas sphaeroides* and *Rhodospseudomonas viridis* as determined by X-ray diffraction, *Proc. Natl. Acad. Sci. U.S.A.* 83, 8589–8593.
- Allen, J. P., Feher, G., Yeates, T. O., Komiya, H., and Rees, D. C. (1987) Structure of the reaction center from *Rhodobacter sphaeroides* R-26: The cofactors, *Proc. Natl. Acad. Sci. U.S.A.* 84, 5730–5734.
- Allen, J. P., Feher, G., Yeates, T. O., Komiya, H., and Rees, D. C. (1987) Structure of the reaction center from *Rhodobacter sphaeroides* R-26: The protein subunits, *Proc. Natl. Acad. Sci. U.S.A.* 84, 6162–6166.
- Ermler, U., Fritzsche, G., Buchanan, S. K., and Michel, H. (1994) Structure of the photosynthetic reaction centre from *Rhodobacter sphaeroides* at 2.65 Å resolution: cofactors and protein-cofactor interactions, *Structure* 2, 925–936.
- Barz, W. P., Vermeglio, A., Francia, F., Venturoli, G., Melandri, B. A., and Oesterhelt, D. (1995) Role of the PufX protein in photosynthetic growth of *Rhodobacter sphaeroides*. 2. PufX is required for efficient ubiquinone/ubiquinol exchange between the reaction center  $Q_B$  site and the cytochrome  $bc_1$  complex, *Biochemistry* 34, 15248–15258.
- Kleinfeld, D., Okamura, M. Y., and Feher, G. (1984) Electron transfer in reaction centers of *Rhodospseudomonas sphaeroides*. I. Determination of the charge recombination pathway of  $D^+Q_AQ_B^-$  and free energy and kinetic relations between  $Q_A^-Q_B$  and  $Q_AQ_B^-$ , *Biochim. Biophys. Acta* 766, 126–140.
- Arata, H. (1985) Free-energy change accompanying the reduction of the reaction center secondary quinone in *Rhodospseudomonas sphaeroides* chromatophores, *Biochim. Biophys. Acta* 809, 284–287.
- Overfield, R. E., Wraight, C. A., and Devault, D. (1979). Microsecond photooxidation kinetics of cytochrome  $c_2$  from *Rhodospseudomonas sphaeroides*: in vivo and solution studies, *FEBS Lett.* 105, 137–142.
- Venturoli, G., Mallardi, A., and Mathis, P. (1993) Electron transfer from cytochrome  $c_2$  to the primary donor of *Rhodobacter sphaeroides* reaction centers. A temperature dependent study, *Biochemistry* 32, 13245–13253.
- Roszak, A. W., Howard, T. D., Southall, J., Gardiner, A. T., Law, C. J., Isaacs, N. W., and Cogdell, R. J. (2003) Crystal structure of the RC-LH1 core complex from *Rhodospseudomonas palustris*, *Science* 302, 1969–1972.
- Mancino, L. J., Dean, D. P., and Blankenship, R. E. (1984) Kinetics and thermodynamics of the  $P870^+Q_A^- \rightarrow P870^+Q_B^-$  reaction in isolated reaction centers from the photosynthetic bacterium *Rhodospseudomonas sphaeroides*, *Biochim. Biophys. Acta* 764, 46–54.
- Palazzo, G., Mallardi, A., Giustini, M., Berti, D., and Venturoli, G. (2000) Cumulant analysis of charge recombination kinetics in bacterial reaction centers reconstituted into lipid vesicles, *Biophys. J.* 79, 1171–1179.

26. Shinkarev, V. P., and Wraight, C. A. (1997) The interaction of quinone and detergent with reaction centers of purple bacteria. I. Slow quinone exchange between reaction center micelles and pure detergent micelles, *Biophys. J.* 72, 2304–2319.
27. Mallardi, A., Palazzo, G., and Venturoli, G. (1997) Binding of ubiquinone to photosynthetic reaction center: determination of enthalpy and entropy changes of the binding process in reverse micelles, *J. Phys. Chem. B* 101, 7850–7857.
28. Baccarini-Melandri, A., and Melandri, B. A. (1971) Partial resolution of the photophosphorylating system of *Rhodospseudomonas capsulata*, *Methods Enzymol.* 23, 556–561.
29. Gray, K. A., Farchaus, J. W., Wachtveitl, J., Breton, J., and Oesterhelt, D. (1990) Initial characterization of site-directed mutants of tyrosine M210 in the reaction centre of *Rhodobacter sphaeroides*, *EMBO J.* 9, 2061–2070.
30. Piazza, R., Pierno, M., Vignati, E., Venturoli, G., Francia, F., Mallardi, A., and Palazzo, G. (2003) Liquid–liquid phase separation of a surfactant-solubilized membrane protein, *Phys. Rev. Lett.* 90, 208101.
31. Bartsch, R. G. (1971) Cytochromes: bacterial, *Methods Enzymol.* 23, 344–363.
32. Palazzo, G., Mallardi, A., Francia, F., Dezi, M., Venturoli, G., Pierno, M., Vignati, E., and Piazza, R. (2004) Spontaneous emulsification of detergent solubilized reaction center: protein conformational changes precede droplet growth, *Phys. Chem. Chem. Phys.* 6, 1439–1445.
33. Venturoli, G., Fernandez-Velasco, J. G., Crofts, A. R., and Melandri, B. A. (1986) Demonstration of a collisional interaction of ubiquinol with the ubiquinol-cytochrome  $c_2$  oxidoreductase complex in chromatophores from *Rhodobacter sphaeroides*, *Biochim. Biophys. Acta* 851, 340–352.
34. Straley, S. C., Parson, W. W., Mauzerall, D. C., and Clayton, R. K. (1973) Pigment content and molar extinction coefficients of photochemical reaction centers from *Rhodospseudomonas sphaeroides*, *Biochim. Biophys. Acta* 305, 597–609.
35. Dutton, P. L., Petty, K. M., Bonner, H. S., and Morse, S. D. (1975) Cytochrome  $c_2$  and reaction center of *Rhodospseudomonas sphaeroides* Ga membranes. Extinction coefficients, content, half-reduction potentials, kinetics and electric field alterations, *Biochim. Biophys. Acta* 387, 536–556.
36. Bowyer, J. R., Meinhardt, S. W., Tierney, G. V., and Crofts, A. R. (1981) Resolved difference spectra of redox centers involved in photosynthetic electron flow in *Rhodospseudomonas capsulata* and *Rhodospseudomonas sphaeroides*, *Biochim. Biophys. Acta* 635, 167–186.
37. Francia, F., Palazzo, G., Mallardi, A., Cordone, L., and Venturoli, G. (2003) Residual water modulates  $Q_A^-$  to  $Q_B$  electron transfer in bacterial reaction centers embedded in trehalose amorphous matrices, *Biophys. J.* 85, 2760–2775.
38. Clayton, R. K. (1966) Spectroscopic analysis of bacteriochlorophylls in vitro and in vivo, *Photochem. Photobiol.* 5, 669–677.
39. McDermott, G., Prince, S. M., Freer, A. A., Hawthornthwaite-Lawless, A. M., Papiz, M. Z., Cogdell, R. J., and Isaacs, N. W. (1995) Crystal structure of an integral membrane light-harvesting complex from photosynthetic bacteria, *Nature* 374, 517–521.
40. Vermeglio, A. (1977) Secondary electron transfer in reaction centers of *Rhodospseudomonas sphaeroides*. Out-of-phase periodicity of two for the formation of ubisemiquinone and fully reduced ubiquinone, *Biochim. Biophys. Acta* 459, 516–524.
41. Wraight, C. A. (1977) Electron acceptors of photosynthetic bacterial reaction centers. Direct observation of oscillatory behaviour suggesting two closely equivalent ubiquinones, *Biochim. Biophys. Acta* 459, 525–531.
42. Palazzo, G., Mallardi, A., Hochkoeppler, A., Cordone, L., and Venturoli, G. (2002) Electron transfer kinetics in photosynthetic reaction centers embedded in trehalose glasses: trapping of conformational substates at room temperature, *Biophys. J.* 82, 558–568.
43. Kleinfeld, D., Okamura, M. Y., and Feher, G. (1984) Electron-transfer kinetics in photosynthetic reaction centers cooled to cryogenic temperatures in the charge-separated state: evidence for light-induced structural changes, *Biochemistry* 23, 5780–5786.
44. Wraight, C. A., Cogdell, R. J., and Clayton, R. K. (1975) Some experiments on the primary electron acceptor in reaction centres from *Rhodospseudomonas sphaeroides*, *Biochim. Biophys. Acta* 396, 242–249.
45. Shinkarev, V. P., and Wraight, C. A. (1993) Electron and proton transfer in the acceptor quinone complex of reaction centers of phototrophic bacteria, in *The Photosynthetic Reaction Center* (Deisenhofer, J., and Norris, J. R., Eds.) Vol. 1, pp 193–255, Academic Press, San Diego.
46. Okamura, M. Y., Isaacson, R. A., and Feher, G. (1975) Primary acceptor in bacterial photosynthesis: obligatory role of ubiquinone in photoactive reaction centers of *Rhodospseudomonas sphaeroides*, *Proc. Natl. Acad. Sci. U.S.A.* 72, 3491–3495.
47. Okamura, M. Y., Debus, R. J., Kleinfeld, D., and Feher, G. (1982) Quinone binding sites in reaction centers from photosynthetic bacteria, in *Functions of Quinones in Energy Conserving Systems* (Trumpower, B. L., Ed.) pp 299–317, Academic Press, New York.
48. Garcia, A. F., Venturoli, G., Gad'on, N., Fernández-Velasco, J. G., Melandri, B. A., and Drews, G. (1987) The adaptation of the electron transfer chain of *Rhodospseudomonas capsulata* to different light intensities, *Biochim. Biophys. Acta* 890, 335–345.
49. Takamiya, K.-I., and Dutton, P. L. (1979) Ubiquinone in *Rhodospseudomonas sphaeroides*. Some thermodynamic properties, *Biochim. Biophys. Acta* 546, 1–6.
50. Crofts, A. R. (1986) Reaction center and  $UQH_2$ :cyt  $c_2$  oxidoreductase act as independent enzymes in *Rps. sphaeroides*, *J. Bioenerg. Biomembr.* 18, 437–445.
51. Crofts, A. R., Meinhardt, S. W., Jones, K. R., and Snozzi, M. (1983) The role of the quinone pool in the cyclic electron transfer chain of *Rps. sphaeroides*: a modified Q-cycle mechanism, *Biochim. Biophys. Acta* 723, 202–218.
52. Fernandez-Velasco, J., and Crofts, A. R. (1991) Complexes or supercomplexes: inhibitor titrations show that electron transfer in chromatophores from *Rps. sphaeroides* involves a dimeric ubiquinol: cytochrome  $c_2$  oxidoreductase, and is delocalized, *Biochem. Soc. Trans.* 19, 588–593.
53. Joliot, P., Vermeglio, A., and Joliot, A. (1989) Evidence for supercomplexes between reaction centers, cytochrome  $c_2$  and cytochrome  $bc_1$  complex, *Biochim. Biophys. Acta* 975, 336–345.
54. Lavergne, J., Joliot, P., and Vermeglio, A. (1989) Partial equilibration of photosynthetic carriers under weak illumination: a theoretical and experimental study, *Biochim. Biophys. Acta* 975, 347–355.
55. Lavergne, J., and Joliot, P. (1991) Restricted diffusion in photosynthetic membranes, *Trends Biochem. Sci.* 16, 129–134.
56. Vermeglio, A., Joliot, P., and Joliot, A. (1993) The rate of cytochrome  $c_2$  photo-oxidation reflects the subcellular distribution of reaction centers in *Rps. sphaeroides* Ga cells, *Biochim. Biophys. Acta* 1183, 352–360.
57. Drachev, L. A., Mamedov, M. D., Mulikidjanian, A. Ya., Semenov, A. Yu., Shinkarev, V. P., and Verkhovsky, M. I. (1989) Transfer of ubiquinol from the reaction center to the  $bc_1$  complex in *Rhodobacter sphaeroides* chromatophores under oxidizing conditions, *FEBS Lett.* 245, 43–46.
58. Crofts, A., Guergove-Kuras, M., and Hong, S. (1998) Chromatophores heterogeneity explains phenomena seen in *Rhodobacter sphaeroides* previously attributed to supercomplexes, *Photosynth. Res.* 55, 357–362.
59. Crofts, A. R. (2000) Photosynthesis in *Rhodobacter sphaeroides*, *Trends Microbiol.* 8, 105.
60. Vermeglio, A., and Joliot, P. (2000) Response from Vermeglio and Joliot, *Trends Microbiol.* 8, 106.
61. Crofts, A. R. (2000) Response from Crofts, *Trends Microbiol.* 8, 107–108.
62. Roth, M., Arnoux, B., Ducruix, A., and Reiss-Husson, F. (1991) Structure of the detergent phase and protein-detergent interactions in crystals of the wild-type (strain Y) *Rhodobacter sphaeroides* photochemical reaction center, *Biochemistry* 30, 9403–9413.
63. Roth, M., Lewit-Bentley, A., Michel, H., Deisenhofer, J., Huber, R., and Oesterhelt, D. (1989) Detergent structure in crystals of a bacterial photosynthetic reaction center, *Nature* 340, 659–661.
64. Gast, P., Hemelrijk, P., and Hoff, A. J. (1994) Determination of the number of detergent molecules associated with the reaction center protein isolated from the photosynthetic bacterium *Rhodospseudomonas viridis*. Effect of the amphiphilic molecule 1,2,3-heptanetriol, *FEBS Lett.* 337, 39–42.
65. McAuley, K. E., Fyfe, P. K., Ridge, J. P., Isaacs, N. W., Cogdell, R. J., and Jones, M. R. (1999) Structural details of an interaction between cardiolipin and an integral membrane protein, *Proc. Natl. Acad. Sci. U.S.A.* 96, 14706–14711.
66. Fyfe, P. K., McAuley, K. E., Roszak, A. W., Isaacs, N. W., Cogdell, R. J., and Jones, R. J. (2001) Probing the interface between membrane proteins and membrane lipids by X-ray crystallography, *Trends Biochem. Sci.* 26, 106–112.



67. Camara-Artigas, A., Brune, D., and Allen, J. P. (2002) Interactions between lipids and bacterial reaction centers determined by protein crystallography, *Proc. Natl. Acad. Sci. U.S.A.* 99, 11055–11060.
68. Schmid, R., and Labahn, A. (2000) Temperature and free energy dependence of the direct charge recombination rate from the secondary quinone in bacterial reaction centers from *Rhodobacter sphaeroides*, *J. Phys. Chem. B* 104, 2928–2936.
69. Allen, J. P., Williams, J. C., Graige, M. S., Paddock, M. L., Feher, G., and Okamura, M. Y. (1998) Free energy dependence of the direct charge recombination from the primary and secondary quinones in reaction centers from *Rhodobacter sphaeroides*, *Photosynth. Res.* 55, 227–233.

BI048629S